DOI: 10.1002/ejic.200900710

Magnesium(II) Complexes of the dpp-BIAN Radical-Anion: Synthesis, Molecular Structure, and Catalytic Activity in Lactide Polymerization

Igor L. Fedushkin,*[a] Alexander G. Morozov,[a] Valentina A. Chudakova,[a] Georgy K. Fukin,[a] and Vladimir K. Cherkasov[a]

Keywords: Magnesium / Redox chemistry / Structure elucidation / Polymerization

Reaction of (dpp-BIAN)Mg(THF)$_3$ (**1**) {dpp-BIAN = 1,2-bis[(2,6-diisopropylphenyl)imino]acenaphthene} with one molar equivalent of 2,2,6,6-tetramethylpiperidine-1-oxyl (TEMPO) proceeds with oxidation of the dpp-BIAN dianion in **1** to the radical-anion and affords the (dpp-BIAN)Mg(TEMPO)(thf) (**2**) complex. The reaction of dpp-BIAN with an excess amount of magnesium and 0.5 molar equivalents of I$_2$ in Et$_2$O gives (dpp-BIAN)MgI(Et$_2$O)$_n$, which then reacts in situ with (Me$_3$Si)$_2$NK to produce (dpp-BIAN)Mg[N(SiMe$_3$)$_2$](Et$_2$O) (**3**). Solvent-free magnesium amide (dpp-BIAN)Mg[N(SiMe$_3$)$_2$] (**4**) was synthesized by treating equimolar amounts of MgI$_2$, dpp-BIAN, and sodium in toluene at reflux followed by treatment with (Me$_3$Si)$_2$NK. Deprotonation of diphenylacetonitrile with [(dpp-BIAN)Mg(μ-Me)]$_2$ (**5**) produces keteniminate complex (dpp-BIAN)Mg(N=C=CPh$_2$)(Et$_2$O) (**6**). Complexes **2**–**4** and **6** were characterized by ESR and IR spectroscopy; their molecular structures were determined by single-crystal X-ray analysis. Compounds **1**–**3** catalyze the ring-opening polymerization of L- and *rac*-lactides to give high molecular weight isotactic and stereoblock polylactides correspondingly.

Introduction

The exceptional reactivity of transition-metal complexes[1–7] of 1,2-bis(arylimino)acenaphthenes (BIANs) is justified by the rigidity and bulkiness as well as the tunable *s*-donor and *p*-acceptor properties of BIANs. Although BIANs were first reported in the 1960s, their use with metals for the formation of complexes only began in the beginning of the 1990s. Transition-metal complexes of neutral BIANs are numerous. Main-group metal derivatives of BIAN ligands, and especially of sterically demanding 1,2-bis[(2,6-diisopropylphenyl)imino]acenaphthene (dpp-BIAN), are also known. In 2003, the ability of dpp-BIAN to act as an "electron sponge" was disclosed. Thus, reduction of dpp-BIAN with sodium resulted in the formation of its mono-, di-, tri-, and tetraanions.[8] The unique stereoelectronic properties of dpp-BIAN allowed the isolation of molecular species with direct Zn–Zn,[9] Zn–Ga,[10] and Li–Ga[11] bonds. Progress in the field of the coordination chemistry of BIAN ligands with s- and *p*-block elements has been reviewed just recently.[12]

One of the focal points of research in coordination chemistry of transition metals is the preparation of robust catalysts for olefin polymerization. Among the most active catalysts for the conversion of ethylene and α-olefins into high molecular weight polymers are nickel BIAN derivatives.[6] In contrast, coordination compounds of main-group metals and of the lanthanides are enthusiastically examined as catalysts for ring-opening polymerization (ROP) of cyclic esters, especially of lactides.[13] Polylactides (PLA), which can be manufactured from renewable plant resources,[14] are very attractive materials, as these are biologically degradable as well as compatible.

The ROP of lactides was developed by the groups of Spassky,[15] Chisholm,[16] Coates,[17] and Gibson.[18] The most active catalytic systems for ROP of cyclic esters consist of aluminum, zinc, yttrium, and magnesium alkoxides and amides supported by N- and O-bi(poly)dentate ligands. A large number of publications on such catalytic systems has appeared over the last years; therefore, only the most recent of them are cited here.[19–22]

In magnesium[23] and aluminum[24] complexes, dpp-BIAN may be present either as a chelating radical-anionic or chelating dianionic ligand (**A** and **B**, respectively). Magnesium complexes with amido/amino[23b,23f,23h] and amido/imino[23j] ligands derived from dpp-BIAN are also reported (**C** and **D**, respectively). As a result of the bulkiness of dpp-BIAN, its monomeric metal complexes are typical, for example, (dpp-BIAN)Mg(thf)$_3$ (**1**),[23a] (dpp-BIAN)Mg*i*Pr(Et$_2$O),[23e] and (dpp-BIAN)AlMe(Et$_2$O).[24d]

Here we report on the syntheses and molecular structures of magnesium *N*-oxide, amide, and ketenimine derivatives

---

[a] G. A. Razuvaev Institute of Organometallic Chemistry, Russian Academy of Sciences
603950 Nizhny Novgorod, Tropinina 49, Russian Federation
Fax: +7-831-462-74-97
E-mail: igorfed@iomc.ras.ru

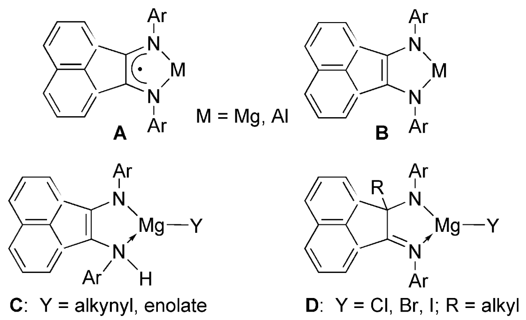

of the dpp-BIAN radical-anion, as well as on catalytic activity of these complexes in the ring-opening polymerization of lactides.

Results and Discussion

Synthesis of (dpp-BIAN)Mg(TEMPO)(thf) (2), (dpp-BIAN)Mg[N(SiMe$_3$)$_2$](Et$_2$O) (3), (dpp-BIAN)Mg[N(SiMe$_3$)$_2$] (4), and (dpp-BIAN)Mg(N=C=CPh$_2$)(Et$_2$O) (6)

Complex **2** was prepared by the reaction of (dpp-BIAN)Mg(thf)$_3$ (**1**) with 2,2,6,6-tetramethylpiperidine-1-oxyl (TEMPO; 1 equiv.). Mixing of the reagents in thf at ambient temperature caused an immediate color change from green-brown (**1**) to cherry-red (**2**), thus indicating oxidation of the dpp-BIAN dianion to the radical-anion (Scheme 1).

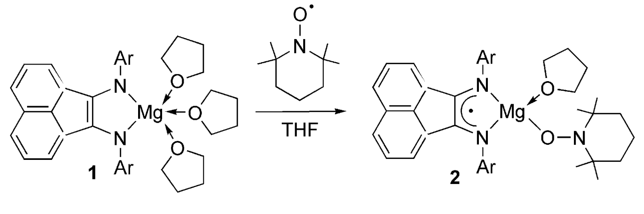

Scheme 1. Synthesis of complex **2**.

The reduction of dpp-BIAN with magnesium in the presence of MgI$_2$ (in situ from Mg and I$_2$; 0.5 equiv.) in diethyl ether produced a cherry-red solution of (dpp-BIAN)MgI(Et$_2$O), which reacted further with (Me$_3$Si)$_2$NK to give complex (dpp-BIAN)Mg[N(SiMe$_3$)$_2$](Et$_2$O) (**3**; Scheme 2).

The solvent-free analog of complex **3**, compound (dpp-BIAN)Mg[N(SiMe$_3$)$_2$] (**4**), was prepared by the reaction of (dpp-BIAN)MgI (in situ from dpp-BIAN, sodium, and MgI$_2$ in toluene) with (Me$_3$Si)$_2$NK (Scheme 2).

The reaction of complex [(dpp-BIAN)Mg(μ-Me)]$_2$[23l] (**5**) with diphenylacetonitrile proceeded with elimination of methane and gave keteniminate derivative (dpp-BIAN)Mg(N=C=CPh$_2$)(Et$_2$O) (**6**; Scheme 3). The process was not accompanied by any visible changes in the color of the reaction mixture, as both **5** and **6** consist of dpp-BIAN radical-anions.

Compounds **2**, **3**, and **6** were isolated by crystallization from diethyl ether in 82, 71, and 70% yield, respectively, whereas compound **4** was isolated by crystallization from toluene in 72% yield. Complexes **2**, **3**, **4**, and **6** are thermally quite robust; they melt in the range 175–215 °C.

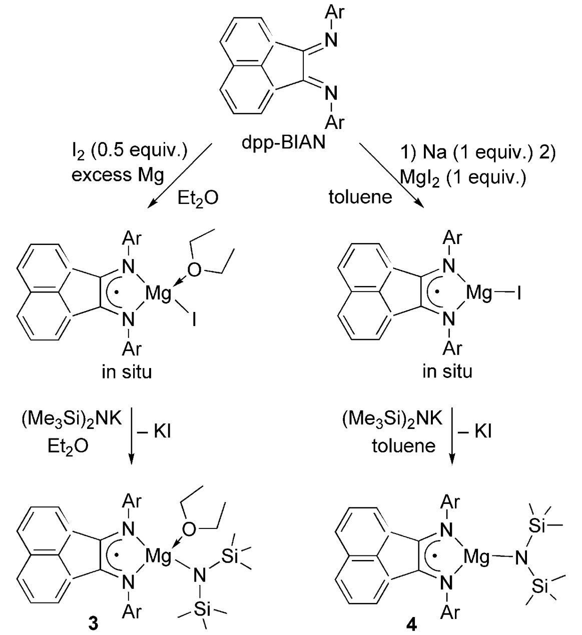

Scheme 2. Synthesis of complexes **3** and **4**.

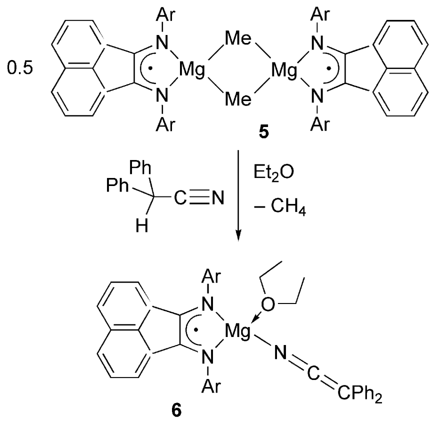

Scheme 3. Synthesis of complex **6**.

However, all four compounds are air and moisture sensitive. Complexes **2**, **3**, **4**, and **6** are paramagnetic in the solid state as well as in solution. Their room-temperature ESR spectra in toluene consist of quintets due to the coupling of the unpaired electron to two ^{14}N nuclei in the dpp-BIAN radical-anion.

Molecular Structures of Compounds 2, 3, 4, and 6

The molecular structures of **2**, **3**, **4**, and **6** were determined by single-crystal X-ray diffraction and are depicted in Figures 1, 2, 3, and 4, respectively. Selected bond lengths and bond angles are presented in Table 1. The unit cell of compound **4** consists of two crystallographically independent molecules. In the unit cell of compound **6** four crystallographically independent molecules are present. Because the geometrical parameters of these molecules in each case are very much alike, the bond lengths and angles for one molecule of **4** and for one molecule of **6** are discussed.

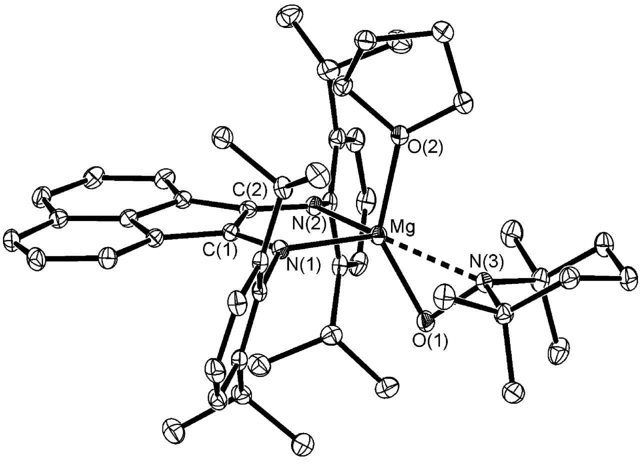

Figure 1. Molecular structure of **2**. The hydrogen atoms are omitted for clarity; thermal ellipsoids are drawn at 30% probability.

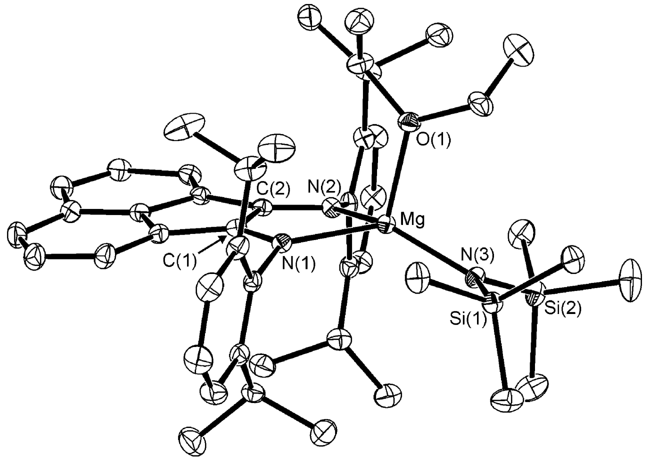

Figure 2. Molecular structure of **3**. The hydrogen atoms are omitted for clarity; thermal ellipsoids are drawn at 40% probability.

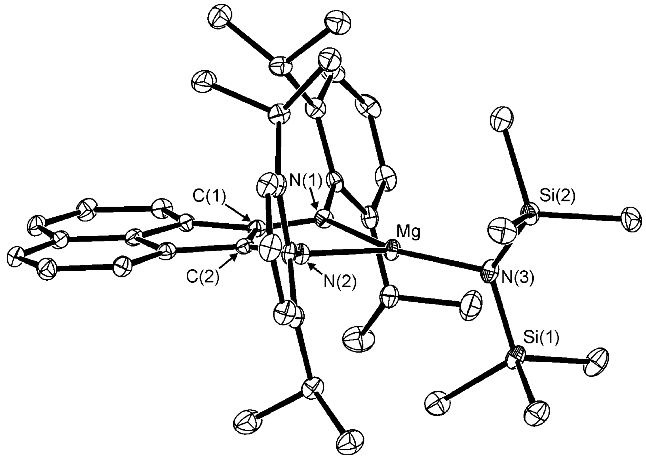

Figure 3. Molecular structure of **4**. The hydrogen atoms are omitted for clarity; thermal ellipsoids are drawn at 30% probability.

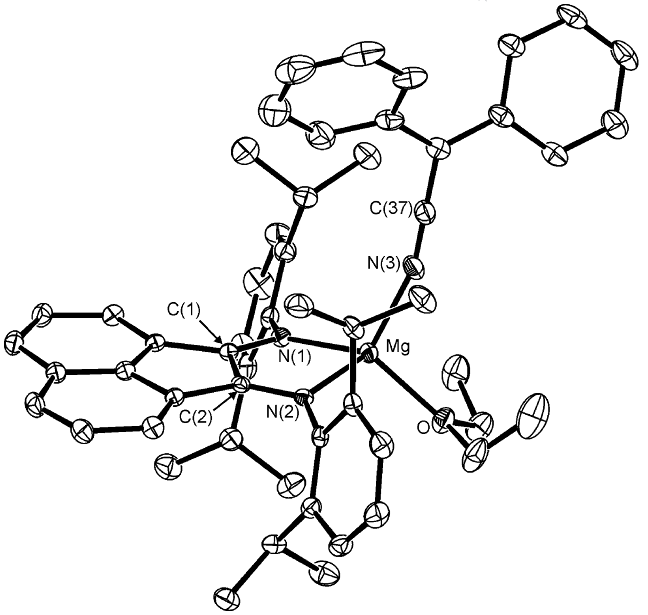

Figure 4. Molecular structure of **6**. The hydrogen atoms are omitted for clarity; thermal ellipsoids are drawn at 30% probability.

Table 1. Selected bond lengths (Å) and angles (°) for **2**, **3**, **4**, and **6**.

	2	**3**	**4**	**6**
Mg–O(1)	1.9061(10)	2.0728(12)		2.0220(9)
Mg–O(2)	2.0617(10)			
Mg–N(1)	2.1280(11)	2.1173(13)	2.057(2)	2.0701(10)
Mg–N(2)	2.1365(11)	2.1366(14)	2.038(2)	2.0606(9)
Mg–N(3)	2.2614(12)	2.0111(13)	1.952(2)	1.9854(9)
Mg–C(1)	2.8446(13)	2.8388(16)	2.755(3)	2.7763(11)
Mg–C(2)	2.8521(13)	2.8414(16)	2.754(3)	2.7762(10)
N(1)–C(1)	1.3345(17)	1.339(2)	1.338(3)	1.3332(13)
N(2)–C(2)	1.3328(16)	1.333(2)	1.331(3)	1.3273(14)
C(1)–C(2)	1.4480(17)	1.439(2)	1.445(4)	1.4460(16)
Mg(1)–Si(1)		3.2340(7)	3.0463(11)	
Mg(1)–Si(2)		3.2111(7)	3.1450(11)	
O(1)–Mg–N(1)	111.50(5)	104.62(5)		
O(1)–Mg–N(2)	114.67(4)	103.75(5)		
N(1)–Mg–N(2)	82.22(4)	82.13(5)	84.98(9)	83.86(4)
N(1)–Mg–N(3)	133.53(5)	128.26(6)	148.54(10)	113.60(4)
N(2)–Mg–N(3)	137.46(4)	131.77(6)	126.48(10)	116.72(5)

Complexes **2**, **3**, and **6** represent monomeric four-coordinate magnesium species, whereas complex **4** contains a three-coordinate magnesium center. In all four compounds the dpp-BIAN ligand is present as a radical-anion. The C–N bond lengths in **2** [1.334(1) and 1.333(1) Å], **3** [1.339(2) and 1.333(2) Å], **4** [1.338(3) and 1.331(3) Å], and **6** [1.333(1) and 1.327(1) Å] are of the same length within estimated standard deviations. However, these distances are longer than those in the free dpp-BIAN [both 1.282(4) Å][25] ligand and in the neutral dpp-BIAN ligand in the molybdenum(0) complex (dpp-BIAN)Mo(CO)$_4$ (av. 1.296 Å).[26] In contrast, the C–N bond lengths in **2**, **3**, **4**, and **6** are shorter than that in the dpp-BIAN dianion in **1** (av. 1.389 Å).[23a]

Until now, seven monomeric magnesium species with a terminal bis(trimethylsilyl)amido ligand (L) have been reported: L$_2$Mg,[27] L$_2$MgPy$_2$,[28] L$_2$Mg(O=C*t*Bu$_2$),[29] (2,4,6-*t*Bu$_3$C$_6$H$_2$S)MgL(thf)$_2$,[30] LMg(BH$_4$)[O(C$_2$H$_4$OMe)$_2$],[31] [(2,6-*i*Pr$_2$C$_6$H$_3$NCMe)$_2$CH]MgL,[32] and [(2-MeOC$_6$H$_4$NCMe)$_2$CH]MgL.[33] The search in the CCDC for complexes with coordination of a TEMPO ligand to magnesium resulted in only $[\{(Me_3Si)_2N\}Mg(\mu\text{-TEMPO})]_2$,[34] which, in contrast to compound **2**, contains a bridging TEMPO group. Structurally characterized magnesium species with a keteneiminate ligand (L′), L′Mg[{(Me$_3$Si)NC(2,6-Me$_2$-C$_6$H$_3$)}$_2$Si(SiMe$_3$)](NCC$_6$H$_3$Me$_2$-2,6)$_2$ and L′Mg[{(Me$_3$Si)-NC(2,6-Me$_2$C$_6$H$_3$)}$_2$Si(SiMe$_3$)](thf)$_2$[35] (L′ = 2,6-Me$_2$-C$_6$H$_4$=C=N), were reported by Lappert and co-workers. As expected, the Mg–N(1) and Mg–N(2) distances in four-coordinate molecules **2** (av. 2.132 Å) and **3** (av. 2.127 Å) are longer than those in three-coordinate complex **4** (av. 2.047 Å).

In **2** and **3**, the coordinative Mg–O(thf) and Mg–O(Et$_2$O) bonds are close [**2**: 2.0617(10); **3**: 2.0728(12) Å], whereas the covalent Mg–O(TEMPO) bond in **2** [1.9061(10) Å] is quite short. Although the distance Mg–N(3) [2.2614(12) Å] in **2** is remarkably longer than the Mg–N(1) and Mg–N(2) bond lengths, the former bond is shorter than the coordinative Mg–N(dpp-BIAN) bonds in complexes of type **C**. For instance, the N→Mg bond in [(dpp-BIAN)(H)]Mg-(CCPh)(thf)[23b] is 2.355(2) Å. Lowering of the metal coordination number on going from **3** to **4** causes a remarkable shortening of the Mg–N(SiMe$_3$)$_2$ bond [**3**: 2.0111(13); **4**: 1.952(2) Å]. Four-coordinate complexes **3** and **6** differ only with respect to the monodentate nitrogen ligands bonded to magnesium atoms. It is interesting that in keteniminate derivative **6** all the metal valent bonds are notably shorter than those in complex **3** (Table 1). This can be explained by the fact that the keteniminate group is less bulky than the (Me$_3$Si)$_2$N ligand.

Polymerization of L- and *rac*-Lactides by using Complexes 1, 2, and 3 as Catalysts

Polylactides (PLA) are biodegradable materials and can be prepared by condensation of lactic acid (LA) or by ring-opening polymerization (ROP) of lactides (Scheme 4). Condensation of lactic acid to give PLA was first reported in 1932.[36] However, this approach can be realized only by using highly pure starting material. In addition, the condensation reaction is reversible, and to shift the equilibrium towards PLA formation the water formed in the course of the process must be removed. In contrast, the ROP of lactides is a thermodynamically favorable reaction (ΔG = –23 kJ mol^{-1}).[37] The ROP of lactides catalyzed by metal complexes was first reported 50 years ago.[38]

One can expect that complexes **1**, **2**, and **3** may act as catalysts in the ROP of lactides because they consist of an oxophilic metal, which as a result of its strong Lewis acidity can coordinate a lactide, and of rigid and bulky diimine ligand, which prevents aggregation of complexes in dimers and provides a definite contour of a free coordination sphere of the metal.

Complexes **1**, **2**, and **3** were examined as catalysts for the ROP of L- and *rac*-lactide in solution as well as in the melt (Table 2). Addition of complex **1** to solutions of *rac*- or L-lactide caused an instant color change from green (**1**) to cherry red, which is a color that is typical for the dpp-BIAN radical-anion, for example, in complexes **2**, **3**, **4**, and **6**. We suggest that in the case of complex **1** lactide acts as one-electron oxidizing agent towards **1**. Such processes have been observed when complex **1** was treated with benzophenone or 9(10*H*)-anthracenone.[23c] In some cases, addition of complexes **1**, **2**, or **3** to solutions of the lactides caused an appearance of a light yellow color of the reaction mixtures, which was indicative of the formation of free dpp-BIAN. In these cases, the oxidative destruction of the complexes is probably caused by impurities present in the commercially available monomers. To reduce the amount of impurities that could still be present in the solvents after their purification by standard methods, the polymerization tests were carried out in solutions with a concentration of the lactides being close to their solubility limits in thf and toluene (ca. 1 mol L^{-1}).

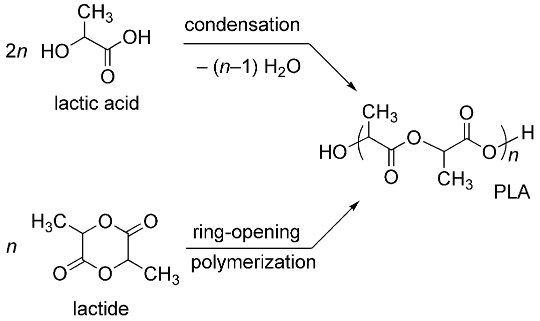

Scheme 4. Two possible synthetic approaches to PLA.

Complexes **1**, **2**, and **3** proved to be very active catalysts of the ROP of L- and *rac*-lactides. Despite some difference between complexes **1**, **2**, and **3**, their catalytic activities are similar. At room temperature, the viscosity of the solutions increased dramatically a few seconds after the addition of the catalysts to a solution of the lactide. An increase in the viscosity of the solution led to a decrease in the polymerization rate: at 20 °C a satisfactory conversion (>90%) was obtained only after 24 h (Table 2, Entries 8 and 12). The calculated and experimental M_n values (Table 2) in these cases differ notably. So far, we have not been able to explain these facts. At 80 °C, a high degree of conversion was achieved after 2 h and experimental M_n values fit much better with calculated ones, at least for the polymerization of L-lactide (Table 2, Entries 1–3). Comparison of Entries 9 and 11 (Table 2) shows that the polymerization rate is higher in thf than in toluene. This can be explained by a better solubility of the lactides and PLA in thf compared to that in toluene and, as a result, a faster diffusion of the monomer to a catalytic center. From this observation it can be concluded that thf does not compete considerably with lactide molecules for the coordination site at the metal centers.

Compounds **1**, **2**, and **3** all catalyze the polymerization of the lactides in melt: representative data for complex **1** are depicted in Table 2. At a relatively low monomer/catalyst ratio (100:1; Table 2, Entry 4) the conversion reached 91%

Table 2. Ring-opening polymerization of L- and *rac*-lactide catalyzed by complexes **1**, **2**, and **3**.

Entry	Complex	[LA]/[Mg]	Medium	[LA] (mol L^{-1})	T (°C)	Time (h)	Conversion (%)	$M_{n,\text{calcd.}}$ ($\times 10^3$)	$M_{n,\text{expt.}}$ ($\times 10^3$)	M_w/M_n
					L-Lactide					
1	**1**	400	thf	1.0	80	2.0	95	54.7	65.4	1.38
2	**2**	400	thf	1.0	80	2.0	>99	57.0	78.7	1.40
3	**3**	400	thf	1.0	80	2.0	93	53.6	57.3	1.46
4	**1**	100	melt	–	195	0.2	91	13.1	23.2	1.82
5	**1**	1000	melt	–	180	2.0	85	122.4	41.1	1.51
6	**1**	2000	melt	–	190	2.0	80	230.4	46.5	1.62
					rac-Lactide					
8	**1**	100	thf	1.0	20	24.0	96	13.8	82.9	1.53
9	**2**	200	thf	1.0	80	1.0	98	28.2	68.8	1.49
10	**2**	500	thf	1.0	80	6.0	89	64.1	116.2	1.65
11	**2**	200	toluene	1.0	80	3.0	94	27.1	59.2	1.40
12	**3**	100	toluene	0.6	20	24.0	>99	14.3	74.5	1.49
13	**1**	860	melt	–	180	14.0	92	113.9	39.7	1.21

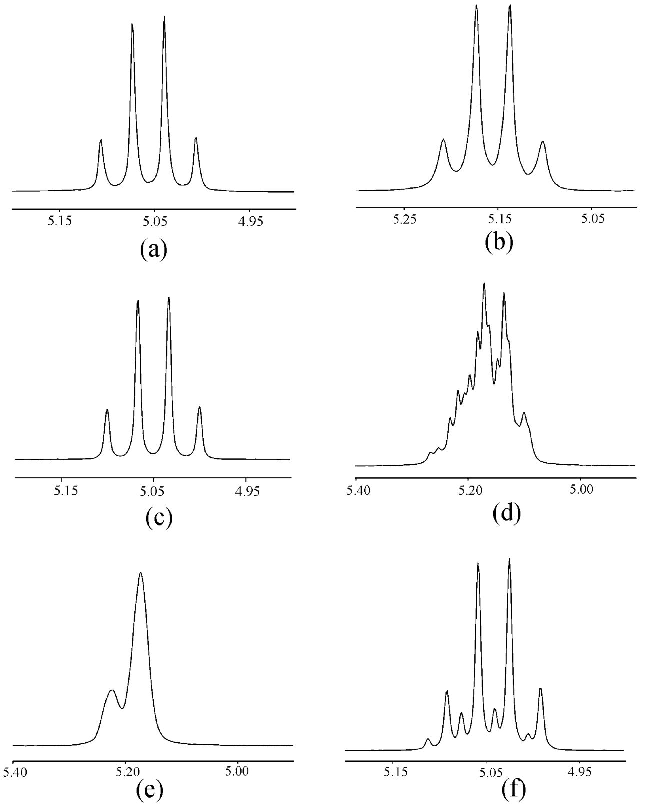

Figure 5. Methine proton signals in the ^{1}H NMR spectra (200 MHz, $CDCl_3$, 293 K, chemical shifts in ppm) of L-lactide (a), poly-L-lactide (b; Table 2, Entry 2), *rac*-lactide (c), poly-*rac*-lactide (d; Table 2, Entry 12), its homodecoupled signal (e), and the mixture of *rac*- and *meso*-lactide (f) formed after thermal depolymerization of poly-*rac*-lactide (d).

after several minutes and afforded PLA with an M_n value higher (23.2×10^3) than that expected (13.1×10^3). This may indicate that the chain-growth process is faster than the chain-initiation reaction. When a larger monomer/catalyst ratio was applied (Table 2, Entries 4 and 6), the experimental M_n values were much lower than the calculated ones. A rough description of these data would be a realization of two concurrent processes: polymerization of LA and depolymerization of PLA. Thus, comparison of Entries 5 and 13 (Table 2) shows that an increase in the polymerization time does not affect the M_n values, although the conversion in the latter case is higher probably because of the higher concentration of the catalysts.

The microstructures of the PLAs obtained by using catalysts **1**, **2**, and **3** were examined by ^{1}H NMR spectroscopy. The region of the methine protons in the ^{1}H NMR spectra of the L- and *rac*-lactides as well as of some polymers obtained thereof are depicted in Figure 5. In all cases, the ROP of L-lactide by using catalysts **1**, **2**, and **3** afforded isotactic poly-L-lactide (PLLA). The signal of the methine protons of PLLA (Figure 5b; Table 2, Entry 2) are ca. 0.11 ppm low-field shifted relative to those of L-lactide (Figure 5a).

The ROP of *rac*-lactide with the use of catalysts **1**, **2**, and **3** gave in all the cases virtually stereoblock polylactides (PLLA-PDLA). Signals of the methine protons of PLLA-PDLA, obtained with the use of complex **3** (Table 2, Entry 12), range from 5.08 to 5.28 ppm (Figure 5d). After homodecoupling, the ^{1}H NMR spectrum revealed two signals centered at $\delta = 5.22$ and 5.16 ppm in a ratio of 1 to 2.8 (Figure 5e). The minor signal corresponds to syndiotactic units, whereas a major one indicates the presence of the isotactic sequences. Thus, an idealized linear progression of stereocenters in PLLA-PDLA, obtained with the use of complex **3** (Table 2, Entry 12), can be envisaged as follows (-*R*-*R*-*R*-*R*-*R*-*R*-*R*-*R*-*S*-*S*-*S*-*S*-*S*-*S*-*S*-*S*-)$_n$. In order to confirm this hypothesis, we carried out a thermal destruction of prepared PLLA-PDLA. It has been suggested that cutting off a chain of the stereoblock polylactide can give either only *rac*-lactide or result also in the formation of *meso*-lactide depending on whether a difference in the strength of ester bonds between *R*-*R* and *R*-*S* is pronounced. Depolymerization was carried in vacuo by gradual heating of the PLLA-PDLA sample to 150 °C over 5 h. Reversion of the polymer to a monomer ensued 89% and gave a mixture of *meso*- and *rac*-lactide in a ratio of 1:5

(Figure 5f). This ratio is different of that expected (*meso*-lactide/*rac*-lactide, 1:7) when thermal cleavage of ester bonds occurs accidentally.

A mixture of *meso*- and *rac*-lactides, formed after thermal destruction of the prepared PLLA-PDLA, was fractionalized by sublimation in vacuo. Recrystallization of pure *meso*- and *rac*-lactides from toluene/hexane and diethyl ether afforded their X-ray quality crystals. The molecular structures of *rac*-lactide (**7**) and *meso*-lactide (**8**) are depicted in Figures 6 and 7, respectively. Selected bond lengths and bond angles are presented in Table 3.

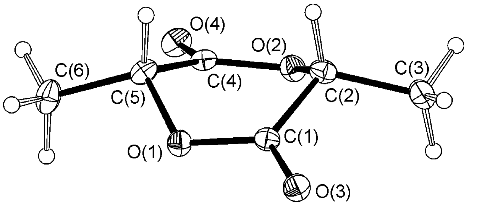

Figure 6. Molecular structure of *rac*-lactide (**7**). Thermal ellipsoids are drawn at 30% probability.

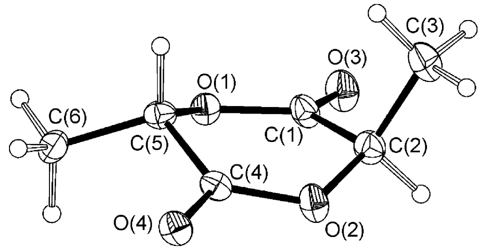

Figure 7. Molecular structure of *meso*-lactide (**8**). Thermal ellipsoids are drawn at 30% probability.

Table 3. Selected bond lengths (Å) and angles (°) for **7** and **8**.

	7	8
O(1)–C(1)	1.340(1)	1.337(3)
O(1)–C(5)	1.462(1)	1.455(3)
O(2)–C(4)	1.341(1)	1.349(3)
O(2)–C(2)	1.461(1)	1.453(3)
O(3)–C(1)	1.200(1)	1.193(3)
O(4)–C(4)	1.198(1)	1.197(3)
C(1)–C(2)	1.515(1)	1.513(4)
C(2)–C(3)	1.503(2)	1.507(4)
C(4)–C(5)	1.509(1)	1.520(4)
C(5)–C(6)	1.503(2)	1.508(4)
C(1)–O(1)–C(5)	117.5(1)	120.5(2)
C(2)–O(2)–C(4)	117.6(1)	122.2(2)

Both **7** and **8** crystallize in the centrosymmetric space group $P2_1/c$ each with four molecules in the unit cell. In the case of **7**, the unit cell consists of two pairs of *R*,*R* and *S*,*S* diastereomers. The six-membered cycles in **7** and **8** have a distorted boat conformation. There is no remarkable difference in the C–C and C–O bond lengths in molecules **7** and **8** (Table 3). However, a difference in the C(1)–O(1)–C(5) and C(2)–O(2)–C(4) bond angles in **7** and **8** (Table 3) indicates that the geometry constrains in these two molecules are not the same.

Conclusions

A use of acenaphthene-1,2-diimine as an ancillary ligand allowed preparation of monomeric magnesium complexes with terminal nitroxide, amide, and keteniminate groups, for example, complexes **2**, **3**, **4**, and **6**. Three different synthetic approaches were exploited: (i) oxidation of a magnesium complex containing the dpp-BIAN dianion; (ii) exchange reactions of magnesium halides supported by the dpp-BIAN radical-anion with alkali metal salts; and (iii) alkane elimination from the alkylmagnesium complex of the dpp-BIAN radical-anion. Complexes **1**, **2**, and **3** proved to be very active catalysts for the ROP of lactides in solution as well as in the melt of monomer. The polymerization rates are higher in thf than in toluene. The ROP of L-lactide with the use of catalysts **1**, **2**, and **3** afforded isotactic PLLA, whereas with *rac*-lactide stereoblock afforded PLAs.

Experimental Section

General Remarks: Starting compounds **1** and **5** as well as newly prepared complexes **2**–**4** and **6** are sensitive to oxygen and moisture. Therefore, all manipulations on the synthesis, isolation, and characterization of **2**–**4** and **6** were carried out in vacuo or under an atmosphere of nitrogen gas by using standard Schlenk technique or in a glove box. The solvents were dried with sodium–benzophenone. *rac*-Lactide (Aldrich) and L-lactide (Nordbiochem) were used without purification. Complex **1** was prepared according to a literature procedure[23a] from dpp-BIAN (0.5 g, 1.0 mmol) and an excess amount of magnesium metal and used in situ for the preparation of complex **2**. The yield of **2** was calculated on the basis of the amount of dpp-BIAN used. Complex **5** was prepared according to a literature procedure.[23l] Solvent-free magnesium diiodide was prepared by desolvation (200 °C, vacuum) of $MgI_2(Et_2O)_n$, which was obtained by treating magnesium metal with iodine in diethyl ether. The melting points were determined in vacuum-sealed capillaries. IR spectra were recorded with a FSM-1201 spectrometer in nujol, whose absorptions are omitted. Size-exclusion chromatography (SEC) of PLAs was performed in thf at 20 °C by using a Knauer Smartline apparatus equipped with Phenogel Phenomenex Columns 5 µm (300 × 7.5 mm) and Security Guard Phenogel Column with RI and UV detectors (254 nm). The flow rate was 2 mL min^{-1}. Columns were calibrated by Phenomenex medium and high molecular weight polystyrene standard kits with peak molecular weights from 3420 to 2570000 Da. ^{1}H NMR spectra were recorded with a Bruker DPX-200 NMR spectrometer; ESR spectra were recorded with a Bruker EMX instrument equipped with an ER 041X microwave bridge.

(dpp-BIAN)Mg(TEMPO)(Et$_2$O) (2): To a solution of complex **1** [in situ from 0.5 g (1.0 mmol) of dpp-BIAN and an excess amount of magnesium metal) in thf (30 mL) was added 2,2,6,6-tetramethylpiperidine-1-oxyl (0.16 g, 1.0 mmol) with stirring. The resulting mixture turned instantly cherry-red. After ca. 10 min, the solvent was evaporated under vacuum. A foamy residue was dissolved in Et_2O (60 mL). Slow evaporation of the solvent gave **2** as deep-red prismatic crystals (0.62 g, 82%). M.p. 194–196 °C. IR (nujol): $\tilde{\nu}$ = 1505 (s), 1430 (s), 1310 (m), 1250 (s), 1180 (s), 1020 (m), 930 (m), 890 (w), 815 (w), 750 (vs), 600 (m), 570 (m), 500 (m), 480 (w) cm^{-1}. ESR (Et_2O, 293 K): *g* = 2.0032, a(^{14}N) = 0.495 mT (2 N). $C_{49}H_{66}MgN_3O_2$ (753.36): calcd. C 78.12, H 8.83; found C 78.05, H 8.71.

Table 4. Crystal data and structure refinement details for **2**–**4** and **6**–**8**.

	2	**3**	**4**
Empirical formula	$C_{49}H_{66}MgN_3O_2$	$C_{46}H_{68}MgN_3OSi_2$	$C_{42}H_{58}MgN_3Si_2$
M_r (g mol^{-1})	753.36	759.52	685.40
Temperature (K)	100(2)	100(2)	100(2)
Crystal system	monoclinic	monoclinic	monoclinic
Space group	$P2_1/n$	$P2_1/c$	$P2_1/c$
a (Å)	10.7060(5)	19.9218(10)	24.4509(10)
b (Å)	18.8014(10)	11.7943(6)	15.5945(7)
c (Å)	21.3581(11)	19.1209(10)	21.4169(9)
α (°)	90	90	90
β (°)	93.0450(10)	99.9900(10)	101.5130(10)
γ (°)	90	90	90
Volume (Å^3)	4293.1(4)	4424.6(4)	8001.9(6)
Z	4	4	8
$\rho_{calcd.}$ (g cm^{-3})	1.166	1.140	1.138
μ (mm^{-1})	0.083	0.131	0.136
$F(000)$	1636	1652	2968
Crystal size (mm)	0.62 × 0.45 × 0.35	0.16 × 0.16 × 0.08	0.43 × 0.35 × 0.30
θ_{min} to θ_{max}	1.91 to 25.00	2.01 to 25.00	0.85 to 25.00
Index ranges	$-12 \le h \le 12$	$-17 \le h \le 23$	$-26 \le h \le 29$
	$-22 \le k \le 12$	$-14 \le k \le 13$	$-18 \le k \le 18$
	$-25 \le l \le 25$	$-21 \le l \le 22$	$-23 \le l \le 25$
Reflections collected	23333	23681	43446
Independent reflections	7554	7788	14096
R_{int}	0.0185	0.0251	0.0433
Max./min. transmission	0.9714/0.9502	0.9896/0.9794	0.9603/0.9437
Data/restraints/parameters	7554/0/760	7788/0/750	14096/0/865
GOF on F^2	1.032	1.052	1.061
Final R indices [$I > 2\sigma(I)$]	$R_1 = 0.0366$	$R_1 = 0.0382$	$R_1 = 0.0568$
	$wR_2 = 0.0987$	$wR_2 = 0.1013$	$wR_2 = 0.1528$
R indices (all data)	$R_1 = 0.0455$	$R_1 = 0.0484$	$R_1 = 0.0877$
	$wR_2 = 0.1034$	$wR_2 = 0.1059$	$wR_2 = 0.1677$
Largest diff. peak/hole (e Å^{-3})	0.281/–0.212	0.512/–0.164	0.556/–0.456
	6	**7**	**8**
Empirical formula	$C_{56}H_{65}MgN_3O_{1.5}$	$C_6H_8O_4$	$C_6H_8O_4$
M_r (g mol^{-1})	828.42	144.12	144.12
Temperature (K)	100(2)	100(2)	100(2)
Crystal system	triclinic	monoclinic	monoclinic
Space group	$P\bar{1}$	$P2_1/c$	$P2_1/c$
a (Å)	20.7186(5)	7.9754(8)	7.7308(8)
b (Å)	23.0320(6)	9.1391(9)	9.8306(11)
c (Å)	24.8794(6)	9.4798(9)	9.3925(10)
α (°)	116.1930(10)	90	90
β (°)	92.0440(10)	106.551(2)	110.039(2)
γ (°)	111.8980(10)	90	90
Volume (Å^3)	9594.2(4)	662.33(11)	670.60(12)
Z	8	4	4
$\rho_{calcd.}$ (g cm^{-3})	1.147	1.445	1.428
μ (mm^{-1})	0.080	0.123	0.122
$F(000)$	3568	304	304
Crystal size (mm)	0.40 × 0.39 × 0.22	0.30 × 0.23 × 0.09	0.40 × 0.24 × 0.08
θ_{min} to θ_{max}	1.97 to 27.50	2.66 to 26.48	2.80 to 26.00
Index ranges	$-26 \le h \le 26$	$-10 \le h \le 8$	$-9 \le h \le 7$
	$-29 \le k \le 29$	$-11 \le k \le 11$	$-12 \le k \le 9$
	$-32 \le l \le 32$	$-8 \le l \le 11$	$-11 \le l \le 11$
Reflections collected	93226	3970	3861
Independent reflections	43690	1362	1318
R_{int}	0.0448	0.0212	0.0174
Max./min. transmission	0.9827/0.9688	0.9890/0.9640	0.9903/0.9529
Data/restraints/parameters	43690/82/2290	1362/0/123	1318/0/91
GOF on F^2	0.916	1.084	1.081
Final R indices	$R_1 = 0.0612$	$R_1 = 0.0390$	$R_1 = 0.0721$
[$I > 2\sigma(I)$]	$wR_2 = 0.1411$	$wR_2 = 0.0949$	$wR_2 = 0.1973$
R indices (all data)	$R_1 = 0.1261$	$R_1 = 0.0442$	$R_1 = 0.0793$
	$wR_2 = 0.1626$	$wR_2 = 0.0978$	$wR_2 = 0.2030$
Largest diff. peak/hole (e Å^{-3})	0.696/–0.654	0.313/–0.147	1.214/–0.347

(dpp-BIAN)Mg[N(SiMe$_3$)$_2$](Et$_2$O) (3): To magnesium shavings (0.48 g, 20 mmol) in Et$_2$O (30 mL) was added iodine (0.13 g, 0.5 mmol). The mixture was stirred at ambient temperature till the color of iodine disappeared completely. To this mixture was added dpp-BIAN (0.5 g, 1.0 mmol). Within 3 h of rigorous stirring, the suspension of dpp-BIAN was completely dissolved, and the reaction mixture turned deep cherry-red. To the filtered solution was added (Me$_3$Si)$_2$NK (0.26 g, 1.0 mmol). The mixture was stirred for 30 min and then filtered. Evaporation of the solvent at ambient temperature afforded complex **3** as deep red crystals (0.54 g, 71 %). M.p. 212–215 °C. IR (nujol): $\tilde{\nu}$ = 1580 (w), 1505 (s), 1310 (w), 1250 (vs), 1180 (s), 1090 (m), 1030 (m), 970 (s), 930 (m), 880 (s), 828 (vs), 810 (s), 760 (s), 740 (s), 650 (s) cm^{-1}. ESR (Et$_2$O, 293 K): g = 2.0029, a(^{14}N) = 0.471 mT (2 N). $C_{46}H_{68}MgN_3OSi_2$ (759.52): calcd. C 72.74, H 9.02; found C 72.12, H 8.79.

(dpp-BIAN)Mg[N(SiMe$_3$)$_2$] (4): A mixture of sodium (0.037 g, 1.6 mmol), dpp-BIAN (0.81 g, 1.6 mmol), and MgI$_2$ (0.45 g, 1.6 mmol) was heated at reflux in toluene (30 mL). After 10 h, the reaction mixture color changed from orange to deep red. To this solution was added (Me$_3$Si)$_2$NK (0.36 g, 1.8 mmol), and the mixture was stirred at 80 °C for 30 min. The red toluene solution was filtered off at ambient temperature. The solution was concentrated at reflux to 10 mL. Cooling the concentrated solution to ambient temperature afforded **4** as deep-red crystals (0.80 g, 72 %). M.p. 200 °C. IR (nujol): $\tilde{\nu}$ = 1523 (s), 1438 (s), 1361 (m), 1311 (m), 1246 (s), 1192 (m), 1107 (s), 1057 (m), 1015 (s), 934 (m), 880 (m), 865 (w), 838 (m), 815 (s), 784 (w), 776 (m), 757 (m), 669 (s), 642 (m), 611 (m), 592 (w), 538 (w), 511 (w), 492 (w), 457 (s), 426 (w), 415 (m) cm^{-1}. ESR (toluene, 293 K): g = 2.0029, a(^{14}N) = 0.415 mT (2 N), a(^{1}H) = 0.130 mT (4 H). $C_{42}H_{58}MgN_3Si_2$ (685.40): calcd. C 73.60, H 8.53; found C 71.23, H 8.06.

(dpp-BIAN)Mg(N=C=CPh$_2$)(Et$_2$O) (6): To a solution of compound **5** (2.16 g, 2 mmol) in diethyl ether was added diphenylacetonitrile (40 mL, 0.38 g, 2 mmol) at –70 °C. A slow increase in the temperature was accompanied by the formation of a gaseous product. After 30 min stirring at room temperature the solution was concentrated to a volume of ca. 10 mL by evaporation of the solvent in vacuo. After 24 h complex **6** was isolated as deep red crystals (1.16 g, 70 %). M.p. 175 °C. IR (nujol): $\tilde{\nu}$ = 1640 (w), 1587 (s), 1528 (s), 1489 (m), 1360 (m), 1312 (m), 1291 (w), 1276 (w), 1253 (m), 1221 (m), 1184 (s), 1150 (m), 1117 (m), 1080 (w), 1042 (w), 1007 (w), 993 (m), 939 (w), 926 (m), 895 (w) cm^{-1}. 857 (w), 835 (s), 819 (s), 803 (m), 786 (s), 773 (m), 752 (vs), 692 (vs), 670 (w), 653 (m), 638 (w), 628 (w), 621 (w), 607 (w), 578 (w), 558 (w), 542 (w), 503 (w), 479 (w), 467 (w), 449 (w), 411 (m) cm^{-1}. ESR (Et$_2$O, 293 K): g = 2.0030, a(^{14}N) = 0.483 mT (2 N). $C_{56}H_{65}MgN_3O_{1.5}$ (828.44): calcd. C 81.19, H 7.91; found C 80.72, H 7.50.

Typical Procedure for the Polymerization of *rac*-Lactide in Solution: In a typical experiment (Table 3, Entry 9), to a suspension of *rac*-lactide (14.4 g, 0.1 mol) in thf (80 mL) at ambient temperature was added a solution of catalyst **2** (0.38 g, 5.0 mmol) in thf (20 mL). The ampoule was sealed under vacuum and stirred with a magnetic stir bar at 80 °C for 1 h. After cooling to ambient temperature the reaction vessel was opened and a small amount of the crude material was taken for determination of monomer conversion by ^{1}H NMR spectroscopy. The polymer was precipitated with an excess amount of methanol, and the solid was filtered off and dried under vacuum to constant weight.

Typical Procedure for the Polymerization of L-Lactide in the Melt: In a typical experiment (Table 3, Entry 4), a glass ampoule (ca. 5 mL) was charged under vacuum with L-lactide (0.92 g, 6.6 mmol) and complex **1** (45 mg, 0.06 mmol). Then, the ampoule was sealed off and placed into an oil bath (150 °C) for 10–12 min. Then, the ampoule was broken and the polymer was extracted with thf (ca. 10 mL). For determination of the conversion of the monomer by ^{1}H NMR spectroscopy, an aliquot of the thf solution was removed by syringe. From the residual thf solution the polymer was precipitated with an excess amount of methanol, and the solid was filtered off and dried under vacuum to a constant weight.

Single-Crystal X-ray Structure Determination of 2, 3, 4, 6, 7, and 8: Crystal data and details of the data collections are listed in Table 4. The intensity data were collected at 100 K with a Bruker SMART APEX diffractometer with the use of graphite-monochromated Mo-K_α (λ = 0.71073 Å) radiation. SADABS[39] was used to perform area-detector scaling and absorption corrections. The structures were solved by direct methods with the use of SHELXS-97[40] and by full-matrix least-squares techniques against F_o^2 by using SHELXL-97.[41] All non-hydrogen atoms were refined anisotropically. The hydrogen atoms were placed in idealized positions and their U_{iso} values were set to ride on the U_{eq} values of the parent carbon atoms [U_{iso}(H) = 1.5 U_{eq} for methyl carbon atoms and 1.2 U_{eq} for other carbon atoms]. The geometrical aspects of the structures were analyzed by using PLATON.[42] CCDC-739304 (for **2**), -739305 (for **3**), -739306 (for **4**), -739307 (for **6**), -739303 (for **7**), and -739302 (for **8**) contain the supplementary crystallographic data for this paper. These data can be obtained free of charge from The Cambridge Crystallographic Data Centre via www.ccdc.cam.ac.uk/data_request/cif.

Acknowledgments

This work was supported by the Russian Foundation for Basic Research and by the Nordbiochem Company.

---

[1] M. W. van Laren, C. J. Elsevier, *Angew. Chem. Int. Ed.* **1999**, *38*, 3715–3717.

[2] a) R. van Belzen, H. Hoffmann, C. J. Elsevier, *Angew. Chem. Int. Ed. Engl.* **1997**, *36*, 1743–1745; b) G. A. Grasa, R. Singh, E. D. Stevens, S. P. Nolan, *J. Organomet. Chem.* **2003**, *687*, 269–279.

[3] A. Heumann, L. Giordano, A. Tenaglia, *Tetrahedron Lett.* **2003**, *44*, 1515–1518.

[4] a) A. E. Cherian, E. B. Lobkovsky, G. W. Coates, *Chem. Commun.* **2003**, *20*, 2566–2567; b) F. Al-Abaidi, Z. Ye, S. Zhu, *Macromol. Chem. Phys.* **2003**, *204*, 1653–1659; c) V. Fassina, C. Ramminger, M. Seferin, R. S. Mauler, R. F. de Souza, A. L. Monteiro, *Macromol. Rapid Commun.* **2003**, *24*, 667–670; d) M. D. Leatherman, S. A. Svejda, L. K. Johnson, M. Brookhart, *J. Am. Chem. Soc.* **2003**, *125*, 3068–3081; e) S. S. Ivanchev, G. A. Tolstikov, V. K. Badaev, N. I. Ivancheva, I. I. Oleinik, S. Ya. Khaikin, I. V. Oleinik, *Vysokomol. Soedin., Ser. A B* **2002**, *44*, 1478–1483 [*Polym. Sci. USSR, Ser. A, B* **2002**, *44*, 931–936 (Engl. Transl.)]; f) C. M. Killian, D. J. Tempel, L. K. Johnson, M. Brookhart, *J. Am. Chem. Soc.* **1996**, *118*, 11664–11665; g) C. Pellecchia, A. Zambelli, M. Mazzeo, D. Pappalardo, *J. Mol. Catal. A* **1998**, *128*, 229–237; h) A. E. Cherian, J. M. Rose, E. B. Lobkovsky, G. W. Coates, *J. Am. Chem. Soc.* **2005**, *127*, 13770–13771; i) J. M. Rose, A. E. Cherian, G. W. Coates, *J. Am. Chem. Soc.* **2006**, *128*, 4186–4187 and references cited therein.

[5] I. Kim, J. M. Hwang, J. K. Lee, C. S. Ha, S. I. Woo, *Macromol. Rapid Commun.* **2003**, *24*, 508–511.

[6] L. K. Johnson, C. M. Killian, M. Brookhart, *J. Am. Chem. Soc.* **1995**, *117*, 6414–6415.

[7] J. C. Alonso, P. Neves, M. J. P. da Silva, S. Quintal, P. D. Vaz, C. Silva, A. A. Valente, P. Ferreira, M. J. Calhorda, V. Felix, M. G. B. Drew, *Organometallics* **2007**, *26*, 5548–5556.

[8] I. L. Fedushkin, A. A. Skatova, V. A. Chudakova, G. K. Fukin, *Angew. Chem. Int. Ed.* **2003**, *42*, 3294–3298.

[9] I. L. Fedushkin, A. A. Skatova, S. Y. Ketkov, O. V. Eremenko, A. V. Piskunov, G. K. Fukin, *Angew. Chem. Int. Ed.* **2007**, *46*, 4302–4305.

[10] I. L. Fedushkin, A. N. Lukoyanov, S. Y. Ketkov, M. Hummert, H. Schumann, *Chem. Eur. J.* **2007**, *13*, 7050–7056.

[11] I. L. Fedushkin, A. N. Lukoyanov, G. K. Fukin, S. Yu. Ketkov, M. Hummert, H. Schumann, *Chem. Eur. J.* **2008**, *14*, 8465–8468.

[12] N. J. Hill, I. Vargas-Baca, A. H. Cowley, *Dalton Trans.* **2009**, 240–253.

[13] a) O. Dechy-Cabaret, B. Martin-Vaca, D. Borissou, *Chem. Rev.* **2004**, *104*, 6147–6176; b) A. Amgoune, C. M. Thomas, J.-F. Carpentier, *Pure Appl. Chem.* **2007**, *79*, 2013–2030; c) A. P. Dove, *Chem. Commun.* **2008**, 6446–6470.

[14] S. Mecking, *Angew. Chem. Int. Ed.* **2004**, *43*, 1078–1085.

[15] N. Spassky, M. Wisniewski, C. Pluta, A. Le Borgne, *Macromol. Chem. Phys.* **1996**, *197*, 2627–2637.

[16] M. H. Chisholm, N. W. Eilerts, *Chem. Commun.* **1996**, 853–854.

[17] T. M. Ovitt, G. W. Coates, *J. Am. Chem. Soc.* **1999**, *121*, 4072–4073.

[18] P. A. Cameron, D. Jhurry, V. C. Gibson, A. J. P. White, D. J. Williams, S. Williams, *Macromol. Rapid Commun.* **1999**, *20*, 616–618.

[19] Aluminum catalysts: a) A. Alaaeddine, C. M. Thomas, T. Roisnel, J.-F. Carpentier, *Organometallics* **2009**, *28*, 1469–1475; b) C.-T. Chen, H.-J. Weng, M.-T. Chen, C.-A. Huang, K.-F. Peng, *Eur. J. Inorg. Chem.* **2009**, 2129–2135; c) H. Du, A. H. Velders, P. J. Dijkstra, Z. Zhong, X. Chen, J. Feijen, *Macromolecules* **2009**, *42*, 1058–1066; d) M. Bouyahyi, E. Grunova, N. Marquet, E. Kirillov, C. M. Thomas, T. Roisnel, J.-F. Carpentier, *Organometallics* **2008**, *27*, 5815–5825; e) M. H. Chisholm, J. C. Gallucci, K. T. Quisenberry, Z. Zhou, *Inorg. Chem.* **2008**, *47*, 2613–2624.

[20] Zinc catalysts: a) Y. Huang, W.-C. Hung, M.-Y. Liao, T.-E. Tsai, Y.-L. Peng, C.-C. Lin, *J. Polym. Sci., Part A: Polym. Chem.* **2009**, *47*, 2318–2329; b) J. Boerner, U. Floerke, K. Huber, A. Doering, D. Kuckling, S. Herres-Pawlis, *Chem. Eur. J.* **2009**, *15*, 2362–2376; c) M. D. Jones, M. G. Davidson, C. G. Keir, L. M. Hughes, M. F. Mahon, D. C. Apperley, *Eur. J. Inorg. Chem.* **2009**, 635–642; d) C. A. Wheaton, B. J. Ireland, P. G. Hayes, *Organometallics* **2009**, *28*, 1282–1285; e) G. Labourdette, D. J. Lee, B. O. Patrick, M. B. Ezhova, P. Mehrkhodavandi, *Organometallics* **2009**, *28*, 1309–1319.

[21] Yttrium catalysts: a) T. V. Mahrova, G. K. Fukin, A. V. Cherkasov, A. A. Trifonov, N. Ajellal, J.-F. Carpentier, *Inorg. Chem.* **2009**, *48*, 4258–4266; b) E. M. Broderick, P. L. Diaconescu, *Inorg. Chem.* **2009**, *48*, 4701–4706; c) Q. Wang, L. Xiang, H. Song, G. Zi, *J. Organomet. Chem.* **2009**, *694*, 691–696.

[22] Magnesium catalysts: a) J. D. Monegan, S. D. Bunge, *Inorg. Chem.* **2009**, *48*, 3248–3256; b) W.-C. Hung, C.-C. Lin, *Inorg. Chem.* **2009**, *48*, 728–734.

[23] a) I. L. Fedushkin, A. A. Skatova, V. A. Chudakova, G. K. Fukin, S. Dechert, H. Schumann, *Eur. J. Inorg. Chem.* **2003**, 3336–3346; b) I. L. Fedushkin, N. M. Khvoinova, A. A. Skatova, G. K. Fukin, *Angew. Chem. Int. Ed.* **2003**, *42*, 5223–5226; c) I. L. Fedushkin, A. A. Skatova, V. K. Cherkasov, V. A. Chudakova, S. Dechert, M. Hummert, H. Schumann, *Chem. Eur. J.* **2003**, *9*, 5778–5783; d) I. L. Fedushkin, A. A. Skatova, A. N. Lukoyanov, V. A. Chudakova, S. Dechert, M. Hummert, H. Schumann, *Russ. Chem. Bull.* **2005**, *53*, 2751–2762; e) I. L. Fedushkin, A. A. Skatova, M. Hummert, H. Schumann, *Eur. J. Inorg. Chem.* **2005**, 1601–1608; f) I. L. Fedushkin, A. G. Morozov, O. V. Rassadin, G. K. Fukin, *Chem. Eur. J.* **2005**, *11*, 5749–5757; g) P. J. Bailey, R. A. Coxall, C. M. Dick, S. Fabre, S. Parsons, L. J. Yellowlees, *Chem. Commun.* **2005**, 4563–4565; h) I. L. Fedushkin, A. A. Skatova, G. K. Fukin, M. Hummert, H. Schumann, *Eur. J. Inorg. Chem.* **2005**, 2332–2338; i) P. J. Bailey, C. M. Dick, S. Fabre, S. Parsons, L. J. Yellowlees, *Dalton Trans.* **2006**, 1602–1610; j) I. L. Fedushkin, V. M. Makarov, E. C. E. Rosenthal, G. K. Fukin, *Eur. J. Inorg. Chem.* **2006**, 827–832; k) I. L. Fedushkin, V. A. Chudakova, M. Hummert, H. Schumann, *Z. Naturforsch., Teil B: Chem. Sci.* **2008**, *63*, 161–168; l) I. L. Fedushkin, A. G. Morozov, M. Hummert, H. Schumann, *Eur. J. Inorg. Chem.* **2008**, 1584–1588.

[24] a) H. Schumann, M. Hummert, A. N. Lukoyanov, I. L. Fedushkin, *Organometallics* **2005**, *24*, 3891–3896; b) I. L. Fedushkin, A. N. Lukoyanov, G. K. Fukin, M. Hummert, H. Schumann, *Russ. Chem. Bull.* **2006**, *55*, 1177–1183; c) A. N. Lukoyanov, I. L. Fedushkin, M. Hummert, H. Schumann, *Russ. Chem. Bull.* **2006**, *55*, 422–428; d) A. N. Lukoyanov, I. L. Fedushkin, H. Schumann, M. Hummert, *Z. Anorg. Allg. Chem.* **2006**, *632*, 1471–1476; e) H. Schumann, M. Hummert, A. N. Lukoyanov, I. L. Fedushkin, *Chem. Eur. J.* **2007**, *13*, 4216–4222.

[25] I. L. Fedushkin, V. A. Chudakova, G. K. Fukin, S. Dechert, M. Hummert, H. Schumann, *Russ. Chem. Bull.* **2004**, *53*, 2744–2750.

[26] I. L. Fedushkin, A. A. Skatova, A. N. Lukoyanov, N. M. Khvoinova, A. V. Piskunov, A. S. Nikipelov, G. K. Fukin, K. A. Lysenko, E. Irran, H. Schumann, *Dalton Trans.* **2009**, 4689–4694.

[27] R. A. Bartlett, M. M. Olmstead, P. P. Power, *Inorg. Chem.* **1994**, *33*, 4800–4803.

[28] G. C. Forbes, A. R. Kennedy, R. E. Mulvey, P. J. A. Rodger, R. B. Rowlings, *J. Chem. Soc., Dalton Trans.* **2001**, 1477–1484.

[29] X. He, J. J. Morris, B. C. Noll, S. N. Brown, K. W. Henderson, *J. Am. Chem. Soc.* **2006**, *128*, 13599–13610.

[30] W. Teng, U. Englich, K. Ruhlandt-Senge, *Inorg. Chem.* **2000**, *39*, 3875–3880.

[31] M. Bremer, G. Linti, H. Noth, M. Thomann-Albach, G. E. W. J. Wagner, *Z. Anorg. Allg. Chem.* **2005**, *631*, 683–697.

[32] A. P. Dove, V. C. Gibson, P. Hormnirun, E. L. Marshall, J. A. Segal, A. J. P. White, D. J. Williams, *Dalton Trans.* **2003**, 3088–3097.

[33] M. H. Chisholm, J. C. Gallucci, K. Phomphrai, *Inorg. Chem.* **2005**, *44*, 8004–8010.

[34] G. C. Forbes, A. R. Kennedy, R. E. Mulvey, P. J. A. Rodger, *Chem. Commun.* **2001**, 1400–1401.

[35] J. D. Farwell, P. B. Hitchcock, M. F. Lappert, A. V. Protchenko, *Chem. Commun.* **2005**, 2271–2273.

[36] W. H. Carothers, G. L. Dorough, F. J. van Natta, *J. Am. Chem. Soc.* **1932**, *54*, 761–772.

[37] A. Duda, S. Penczek, *Macromolecules* **1990**, *23*, 1636–1639.

[38] J. Kleine, H.-H. Kleine, *Makromol. Chem.* **1959**, *30*, 23–38.

[39] G. M. Sheldrick, *SADABS: Empirical Absorption Correction Program*, University of Göttingen, **1996**.

[40] G. M. Sheldrick, *SHELXS-97: Program for Crystal Structure Solution*, University of Göttingen, **1990**.

[41] G. M. Sheldrick, *SHELXL-97: Program for Crystal Structure Refinement*, University of Göttingen, **1997**.

[42] A. L. Spek, *PLATON: A Multipurpose Crystallographic Tool*, Utrecht University, **2000**.

Received: July 24, 2009